Journal of Power Sources 195 (2010) 4444–4457

Contents lists available at ScienceDirect

Journal of Power Sources

journal homepage: www.elsevier.com/locate/jpowsour

Influence of expander components on the processes at the negative plates of lead-acid cells on high-rate partial-state-of-charge cycling. Part II. Effect of carbon additives on the processes of charge and discharge of negative plates

D. Pavlov*, P. Nikolov, T. Rogachev

Institute of Electrochemistry and Energy Systems, Bulgarian Academy of Sciences, Acad. Georgi Bonchev Street, bl. 10, Sofia 1113, Bulgaria

ARTICLE INFO

Article history:
Received 13 November 2009
Received in revised form
29 December 2009
Accepted 30 December 2009
Available online 15 January 2010

Keywords:
Lead-acid battery
Expander in lead-acid battery
Negative plate of lead-acid battery
Active carbon
Carbon black additive

ABSTRACT

Lead-acid batteries operated in the high-rate partial-state-of-charge (HRPSoC) duty rapidly lose capacity on cycling, because of sulfation of the negative plates. As the battery operates from a partially discharged state, the small $PbSO_4$ crystals dissolve and precipitate onto the bigger crystals. The latter have low solubility and hence $PbSO_4$ accumulates progressively in the negative plates causing capacity loss. In order to suppress this process, the rate of the charge process should be increased.

In a previous publication of ours we have established that reduction of Pb^{2+} ions to Pb may proceed on the surface of both Pb and carbon black particles. Hence, the reversibility of the charge–discharge processes improves, which leads to improved cycle life performance of the batteries in the HRPSoC mode. However, not all carbon forms accelerate the charge processes. The present paper discusses the electrochemical properties of two groups of carbon blacks: Printex and active carbons. The influence of Vaniseprse A and $BaSO_4$ (the other two components of the expander added to the negative plates) on the reversibility of the charge–discharge processes on the negative plates is also considered. It has been established that lignosulfonates are adsorbed onto the lead surface and retard charging of the battery. $BaSO_4$ has the opposite effect, which improves the reversibility of the processes on cycling and hence prolongs battery life in the HRPSoC duty. It has been established that the cycle life of lead-acid cells depends on the type of carbon black or active carbon added to the negative plates. When the carbon particles are of nano-sizes (<180 nm), the HRPSoC cycle life is between 10,000 and 20,000 cycles. Lignosulfonates suppress this beneficial effect of carbon black and activated carbon additives to about 10,000 cycles. Cells with active carbons have the longest cycle life when they contain also $BaSO_4$ but no lignosulfonate. A summary of the effects of the three expander components on the elementary processes during charge of negative lead-acid battery plates is presented at the end of the paper.

1. Introduction

Batteries in hybrid electric vehicles operate under high-rate partial-state-of-charge (HRPSoC) conditions, namely:

(a) The battery is in partially discharged state during cycling, which creates favourable conditions for a $PbSO_4$ recrystallization process to proceed, i.e. small $PbSO_4$ crystallites dissolve and precipitate onto the big $PbSO_4$ crystals. This leads to progressive sulfation of the negative plates. On the positive plates, the discharge processes proceed in the hydrated zones of PbO_2 particles through a series of chemical reactions which retard substantially the formation and growth of big $PbSO_4$ crystals [1]. Moreover, the process of sulfation is impeded by the small pore radii in the lead dioxide active mass. Hence, the sulfation issue is confined to the negative plates only.

(b) Cycling in the HRPSoC mode comprises very short charge and discharge pulses (micro-cycles) resulting in only 1–3% depth of discharge (DOD). In order to sustain the battery in charged state, the charge and discharge processes should be fully reversible. As the negative plates are subject to rapid sulfation, the charge processes should be accelerated to such an extent that the whole amount of $PbSO_4$ formed during discharge could be converted back to lead during the re-charge cycle.

(c) Both battery charge and discharge are conducted at high rates (with high currents of 2–5*C* A). This results in high polarization of the negative electrodes, which may lead to some side reactions of water decomposition and evolution of hydrogen and oxygen. Consequently, the efficiency of charge will be reduced and the rate of sulfation will increase.

* Corresponding author. Tel.: +359 2 971 00 83; fax: +359 2 873 15 52.
E-mail address: dpavlov@labatscience.com (D. Pavlov).

0378-7753/$ – see front matter © 2010 Elsevier B.V. All rights reserved.
doi:10.1016/j.jpowsour.2009.12.132

Table 1
Carbon materials under investigation.

Product	Manufacturer	Type of material	Signature	Specific characteristics	
				Particle size	BET surface
PRINTEX® series					
PRINTEX® A	Degussa	Carbon black	PR1	41 nm	45 $m^2 g^{-1}$
PRINTEX® U	Degussa	Carbon black	PR2	25 nm	100 $m^2 g^{-1}$
PRINTEX® F85	Degussa	Carbon black	PR3	16 nm	200 $m^2 g^{-1}$
PRINTEX® 90	Degussa	Carbon black	PR4	14 nm	300 $m^2 g^{-1}$
Electrochemically active carbons (EACs)					
NORIT AZO	NORIT	Activated carbon	AC1	100 μm	635 $m^2 g^{-1}$
VULCAN XC72R	Cabot Corporation	Carbon black	AC2	30 nm	257 $m^2 g^{-1}$
Black Pearls 2000	Cabot Corporation	Carbon black	AC3	12 nm	1475 $m^2 g^{-1}$
PRINTEX® XE2	Degussa	Carbon black	AC4	30 nm	910 $m^2 g^{-1}$

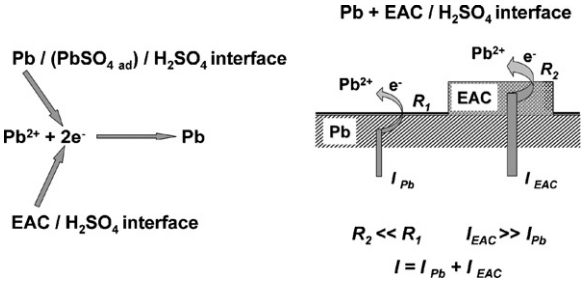

Fig. 1. Parallel mechanism of reduction of Pb^{2+} ions to Pb on the lead and carbon surfaces.

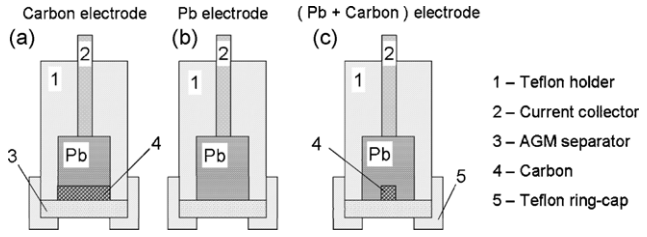

Fig. 2. Model electrodes used to investigate the electrochemical processes taking place on the Pb and carbon surfaces. 1, Teflon holder; 2, current collector; 3, AGM separator; 4, carbon; 5, Teflon ring-cap.

It has been established that the negative plates of lead-acid batteries cycled with 1 min charge and 1 min discharge pulses at a current rate of 2*C*A lose capacity and the battery discharges fully after between 1300 and 1800 micro-cycles.

Nakamura, Shiomi et al. [2,3] have found that introduction of increased amounts of carbon black to the negative paste retards substantially the sulfation of the negative plates on HRPSoC cycling and the number of completed micro-cycles increases to about 5000. The authors explain the observed effect of carbon black with the formation of a conductive network of carbon around the $PbSO_4$ crystals, which is evidenced by scanning electron microscopy of the negative active mass (NAM). Hollenkamp et al. [4] have established, within a project of the Advanced Lead-Acid Battery Consortium (ALABC) program, that addition of graphite or carbon black to the negative paste improves notably its conductivity and lowers the charge voltage of the cells. Calabek et al. [5] have proved that the presence of carbon in NAM reduces its pore radii and thus impedes the continuous growth of $PbSO_4$ crystals, sustaining formation of small crystallites of high solubility and hence efficient charge process. Lam et al. [6] have pointed out that certain carbon forms (depending on the initial product from which they have been produced) may contain impurities which would lower the overpotential of hydrogen evolution and eventually reduce the efficiency of charge. Newnham et al. [7] have found that the specific surface area of NAM is an important parameter as it sustains the potential of the negative plates below the hydrogen evolution potential. However, not all carbon forms that increase the specific surface of NAM contribute to improvement of battery cycle life on HRPSoC operation. Moseley [8] assumes that carbon acts as an electro-osmotic pump that facilitates acid diffusion in the inner NAM volume at high rate of charge and discharge. Lam et al. [9–11] have created an ultra-battery with a conventional PbO_2 positive plate and a negative plate comprising two parts: half of it is a carbon electrode and the other half is a regular negative plate (with sponge lead active material). In the ultra-battery design, carbon is in electrical, but not in physical contact with the negative active material. It has been speculated that only those mechanisms of carbon action which could still operate when the carbon is isolated from the lead active mass can be considered as candidates for providing the major benefit to charge efficiency and impeding negative plate sulfation. Moseley [12] has suggested that capacitive phenomena occur when the lead active mass contains considerable amounts of carbons. During charge with high currents, the electric double layer on the carbon surface is charged first. This process takes place at potentials between the stationary Pb electrode potential and the potential of hydrogen evolution. The electric double layer is discharged slowly at the expense of reduction of $PbSO_4$ to Pb. Thus, "the capacitive element can support charge and discharge events that occur at the highest rates, and the Faradaic part of the cell can cope with events that take place over a longer timescale."

In a previous investigation of ours into the electrochemical properties of active carbons [13] we have established that the electrochemical reaction of reduction of Pb^{2+} ions to Pb proceeds not only on the lead surface, but also on the surface of carbon particles. The parallel mechanism of the electrochemical reactions of charge of negative battery plates is presented diagrammatically in Fig. 1.

The specific surface of the carbon phase is larger than that of the lead phase. Hence, the charge reaction is accelerated and the number of completed micro-cycles increases substantially. To be able

Table 2
Printex carbons particle sizes measured from Fig. 3.

Product	Signature	Carbon particle size range	Average carbon particle size
PRINTEX® A	PR1	100–150 nm	125 nm
PRINTEX® U	PR2	80–100 nm	90 nm
PRINTEX® F85	PR3	70–90 nm	80 nm
PRINTEX® 90	PR4	70–90 nm	80 nm

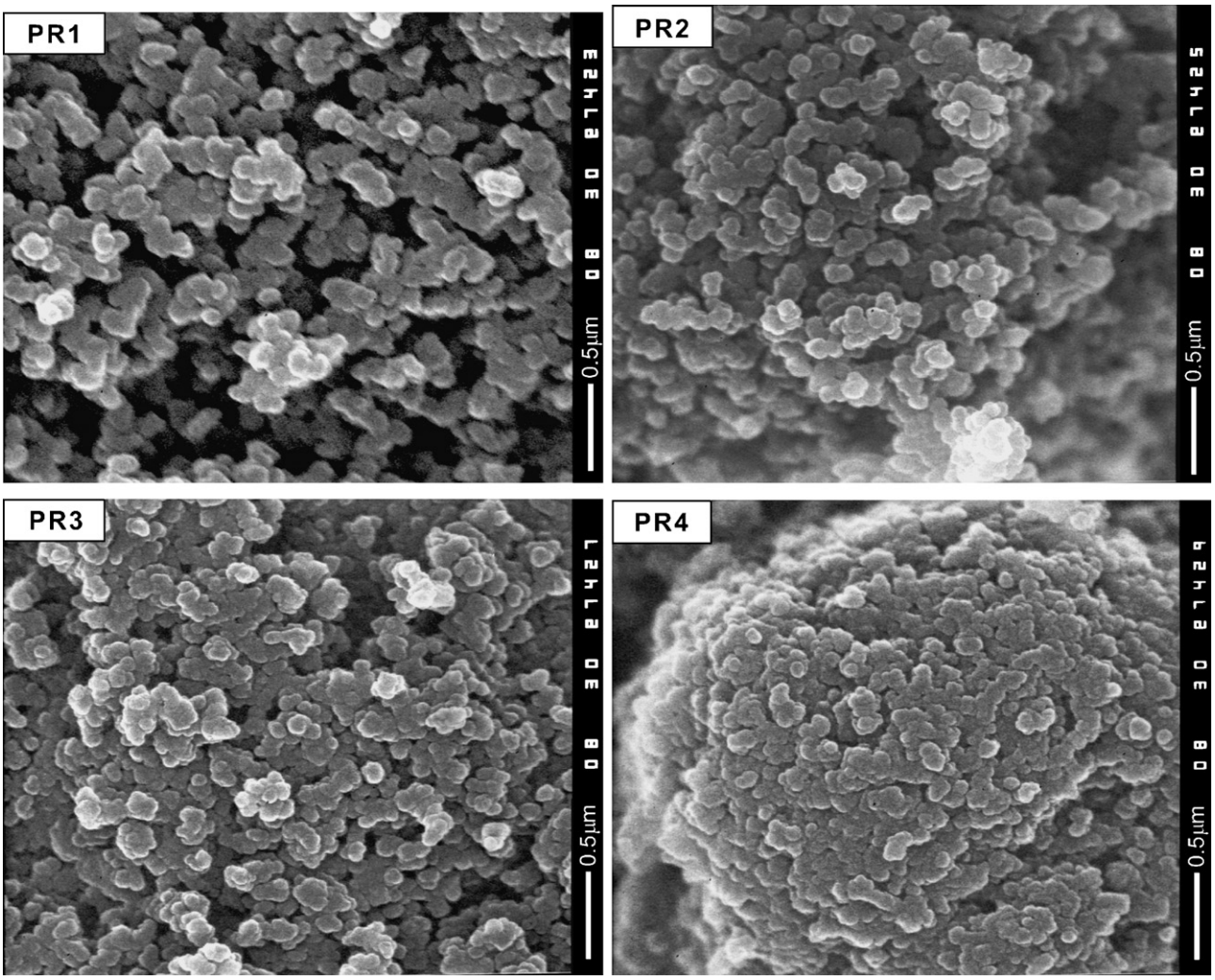

Fig. 3. SEM micrographs of the structure of Printex carbon black particles.

to exhibit this effect, carbons should have high affinity to lead so as to ensure good electron contact between the lead and carbon particles. Moreover, carbons should have high electro-conductivity to allow charging of the double layer. The potential barrier of electron transfer to Pb^{2+} ions through the carbon/solution interface should be low. And finally, carbons should have high specific surface, i.e. small particle size. We called these carbon materials *electrochemically active carbons* (*EACs*). This means that not all types of carbon additives are able to enhance the charge process and make the charge–discharge reactions more reversible.

The present paper will discuss the electrochemical behaviour of two groups of carbon blacks with small particle sizes on HRPSoC cycling. Special attention will be given to the influence of the other two expander components (lignosulfonate and $BaSO_4$) on the effect of carbons. The correlation between carbon particle size and number of completed HRPSoC cycles will be examined as well.

2. Experimental

2.1. Carbon additives to the negative active mass

For the purpose of the present investigation we selected two types of commercially available carbon materials. The basic characteristics of the selected carbon products, as specified by the manufacturers, are summarized in Table 1.

As evident from the table, carbon blacks of the PRINTEX® series and electrochemically active carbons have particle sizes within the nano-range.

In an attempt to disclose the mechanism(s) by which carbon additives improve the charge acceptance of the negative plates and extend the cycle life of lead-acid cells operated under HRPSoC regime we studied the *influence of carbon concentration* in NAM on the electrochemical behaviour of the negative plates and on the performance of the test cells. Negative plates were prepared with each type of carbon additive selected for the investigation, varying its amount in five different concentrations, and these plates were tested. In this way we varied the electrochemically active surface of NAM and followed the resultant changes in the electrochemical parameters of the negative plates of lead-acid cells cycled under HRPSoC conditions.

2.2. Lead-acid test cells

The technology of preparation of pastes with different additive concentrations, as well as details about the fabrication of the negative plates and the test cell design characteristics, were discussed in Part I of the present work [14], so we will not repeat these descriptions here.

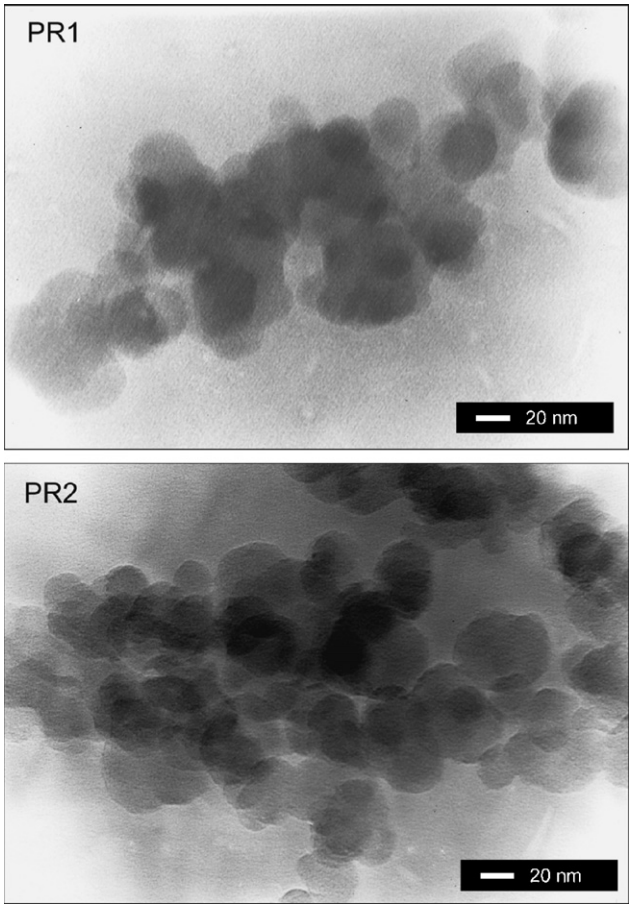

Fig. 4. Transmission electron microscope (TEM) images of Printex 1 and 2 carbon blacks. Magnification 400,000×.

2.3. Electrical parameters of the test cells

First, the initial capacity of the cells was determined at 20-h discharge rate, followed by Peukert tests. Finally, the cells were set to cycle life test under simulated high-rate partial-state-of-charge (HRPSoC) regime. The specific conditions under which the above measurements and tests were conducted were also presented in Part I of this investigation [14], we will not get into these details in the present paper. We will remind only that the simulated HRP-SoC cycling profile comprised the following micro-cycles: charge at 2*C* rate for 60 s, rest for 10 s, discharge at 2*C* rate for 60 s, rest for 10 s (*C* is the capacity after 1 h discharge determined from the Peukert dependence). The cell voltage was measured at the end of the charge or discharge micro-cycles and the test was stopped when the end-of-discharge voltage fell down to 1.83 V or when the end-of-charge voltage reached an upper limit of 2.83 V. The above described cycling steps comprised one cycle-set of the test. The cells were re-charged to 100% SoC and their C_{20} capacity was measured after this cycle-set. Then the cells were discharged with 1*C* A to 50% SoC and a new cycle-set was conducted. The conditionally assumed end-of-cycle life criterion was when the cells failed to complete 4000 micro-cycles within one cycle-set.

2.4. Model electrodes

The model electrodes used in this investigation were developed in the course of previous studies of ours [13,15] and were further modified for the experiments described in Part I of this work [14]. The modified design of the model electrodes used to investigate the influence of carbons on the HRPSoC behaviour of lead-acid cells is presented diagrammatically in Fig. 2.

Three types of model electrodes (ME) were used:

(a) *Carbon electrode*. The base of the Pb–0.1%Ca spine, inserted in a PTFE holder, is covered with a layer of carbon. A sheet of

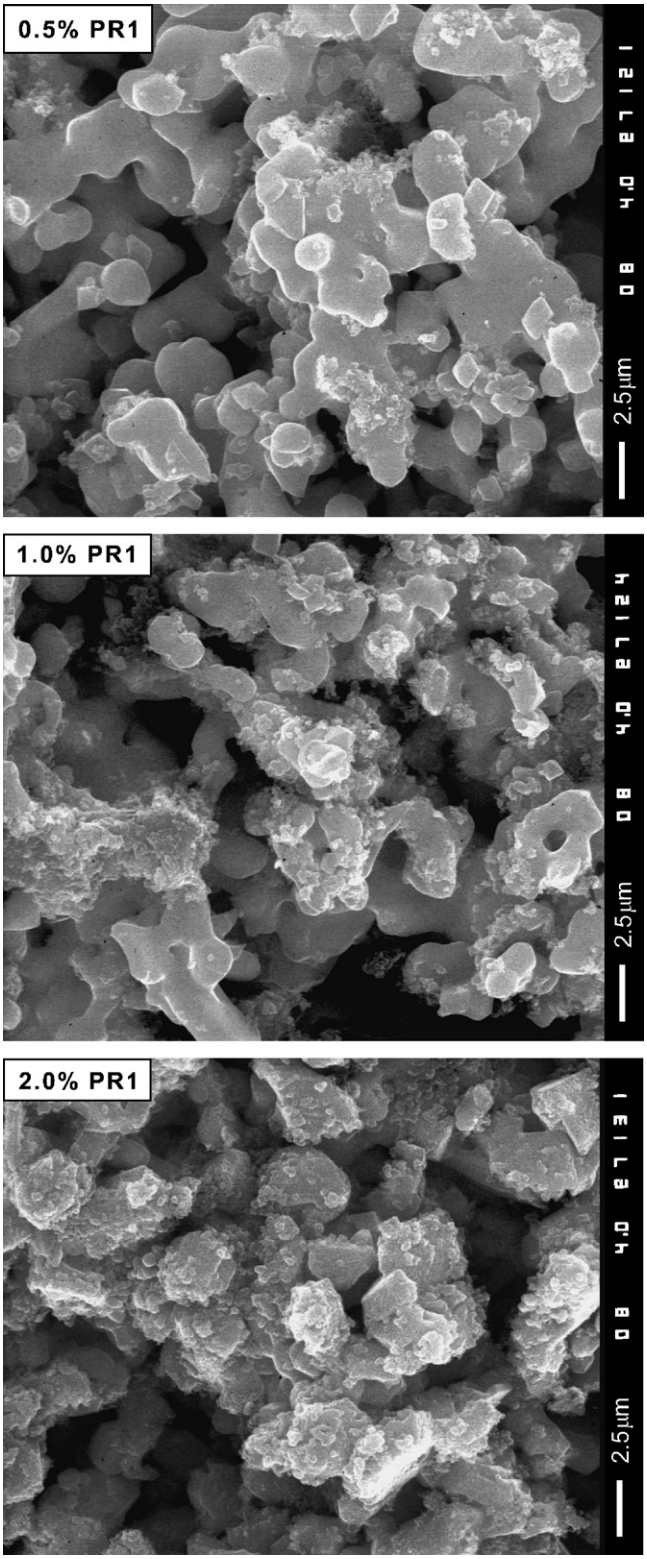

Fig. 5. SEM micrographs of negative active mass containing 0.8% $BaSO_4$ and three different concentrations of PR1 carbon black: 0.5%, 1.0% or 2.0% PR1.

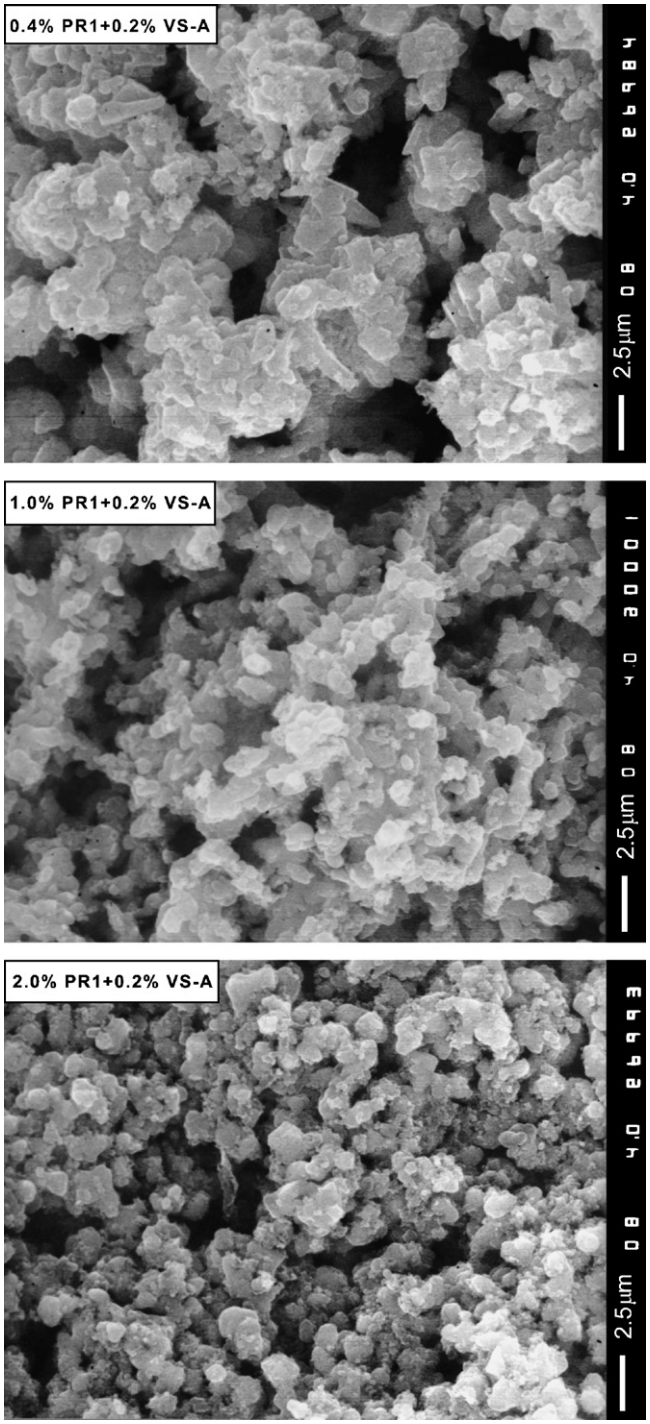

Fig. 6. SEM micrographs of negative active mass containing: 0.2% Vanisperse A, 0.8% $BaSO_4$ and three different concentrations of PR1 carbon black: 0.5%, 1.0% or 2.0% PR1.

AGM separator is placed over the investigated carbon layer and pressed with a PTFE ring-cap. This electrode design confines transfer of carbon material from the ME to the electrolyte.

(b) *Pb electrode*. It comprises a Pb–0.1%Ca spine, inserted in a PTFE holder, covered with an AGM separator and pressed with a PTFE ring-cap. This model electrode behaves as a $Pb/PbSO_4$ electrode during the volt-ampere tests.

(c) (*Pb + C*) *electrode*. This electrode is of the same design as the above Pb model electrode, but there is a small cavity in the center of the Pb spine base which is filled with carbon material. Again, the electrode surface is covered with an AGM separator sheet and pressed with PTFE ring-cap. The AGM sheet prevents the carbon material from dissolving in the electrolyte. This electrode is used to demonstrate the processes that proceed simultaneously on the surfaces of both Pb and carbon phases, i.e. to study the behaviour of the two electrode parts: capacitor and Faraday electrodes.

3. Experimental results and discussion

3.1. Carbon blacks of the Printex series: PR1, PR2, PR3, and PR4

3.1.1. Structure of PR particles and of NAM with addition of PR carbons

Fig. 3 presents SEM pictures of four types of Printex carbon black particles labeled as PR1, PR2, PR3 and PR4, respectively. Several particles are interconnected into agglomerates (PR1, PR2, and PR3) and the agglomerates are interconnected to form a network. The SEM image of the PR4 carbon sample features better bonding between the particles in agglomerates and the agglomerates interconnected into aggregates of considerable size.

From the above SEM images we determined the sizes of the different carbon particles (agglomerates). Some of them comprise several smaller particles. Table 2 presents the obtained particle size values for the four types of Printex carbons.

A comparison between these values and the particle sizes summarized in Table 1 indicates that the Printex carbons used in this study seem to have particle sizes bigger by a factor of 2.8 (for PR1) to 5.7 (for PR4) than the sizes specified by the manufacturers. In an attempt to resolve this discrepancy, the Printex carbons were examined by a transmission electron microscope at 400,000× magnification. The carbon samples were subjected to vibration sputtering prior to the TEM examination. Fig. 4 shows the obtained TEM images of PR1 and PR2 carbons.

The pictures show clearly that the carbon particles are actually built of a number of smaller grains that are well interconnected (agglomerated). A special study should be performed with the aim to elucidate in more detail the structure of carbon particles and the specific influence of its components on the properties of the carbon material.

During preparation of the pastes some exothermic reactions proceed between PbO and H_2SO_4 causing the paste temperature to rise to 50–60 °C. The paste is stirred continuously for 30 min, which generates friction among the particles of the viscous paste mass. It can be presumed that, as a result of this friction, both the agglomerates built of carbon particles and the PR4 aggregates will be broken into individual particles, or small groups of particles, during preparation of the paste. Thus, the agglomerated carbon particles will be separated from one another in the final paste and in the negative active mass formed.

Fig. 5 shows SEM images of negative active mass samples containing 0.8% $BaSO_4$ and PR1 carbon added in three different concentrations: 0.5%, 1.0% or 2.0% PR1 by weight versus the leady oxide (LO) used for paste preparation. The pictures feature a skeleton lead structure. PR1 particles have adsorbed on some parts of the skeleton surface. In the NAM with 0.5% PR1, the PR1 particles have adsorbed to the edges and apexes of the skeleton branches. With increase of the PR1 load in NAM, the coverage of the lead skeleton surface with PR1 particles increases (see SEM pictures of NAM with 1.0% or 2.0% PR1). Consequently, the free lead surface diminishes significantly and the carbon surface becomes dominating. On grounds of the SEM data it can be generally concluded that the appearance of the lead skeleton structure does not change much with increase of the PR1 concentration in NAM.

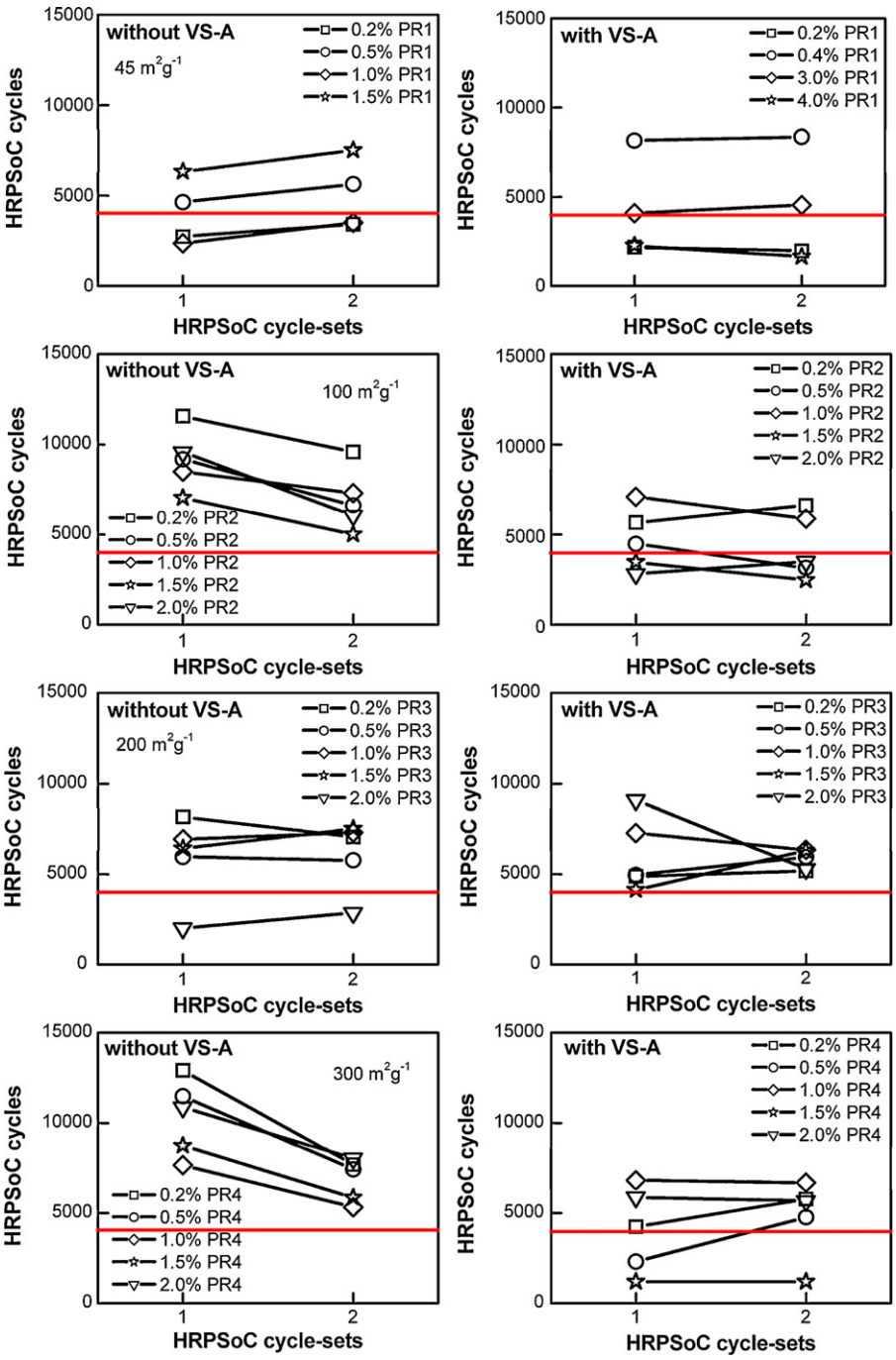

Fig. 7. Completed HRPSoC cycles, within two cycle-sets, for cells with different amounts of PR1-4 in NAM, with or without VS-A.

This is not the case, however, when besides PR1 carbon black, Vanisperse A (0.2%) is also added to the paste. SEM pictures of NAM with PR1 and 0.2% VS-A are presented in Fig. 6.

Here again PR1 particles adsorbed on the lead skeleton can be seen, but the thickness of the skeleton branches decreases with increase of PR1 concentration in NAM. These results imply that the combination of PR1 and VS-A affects the process of lead crystallization. Such an effect of lignosulfonate has been observed and described earlier [16]. The cross-section through the lead skeleton branches is reduced, which will cause the ohmic resistance in some parts of the plate to increase and will eventually decrease the number of cycles at 2*C* rate that the cell will complete within one cycle-set of the HRPSoC test.

3.1.2. HRPSoC cycling tests of cells with Printex and VS-A additives to NAM

Fig. 7 presents the number of completed cycles, within two cycle-sets of the HRPSoC test, for cells with different content of Printex carbon blacks (PR1 to PR4) in NAM, with or without Vanisperse. The conditional cycle life limit of 4000 cycles per cycle-set is also marked in the figure.

The four types of PR carbons affect the charge–discharge processes on HRPSoC cycling in different ways. The concentration of the additives in NAM is of special importance. Thus, the cells with PR2 or PR4 but without VS-A complete more than 4000 cycles in each of the two cycle-sets, irrespective of the PR loading level. The cells with PR1 complete more than 4000 cycles at PR1 concentra-

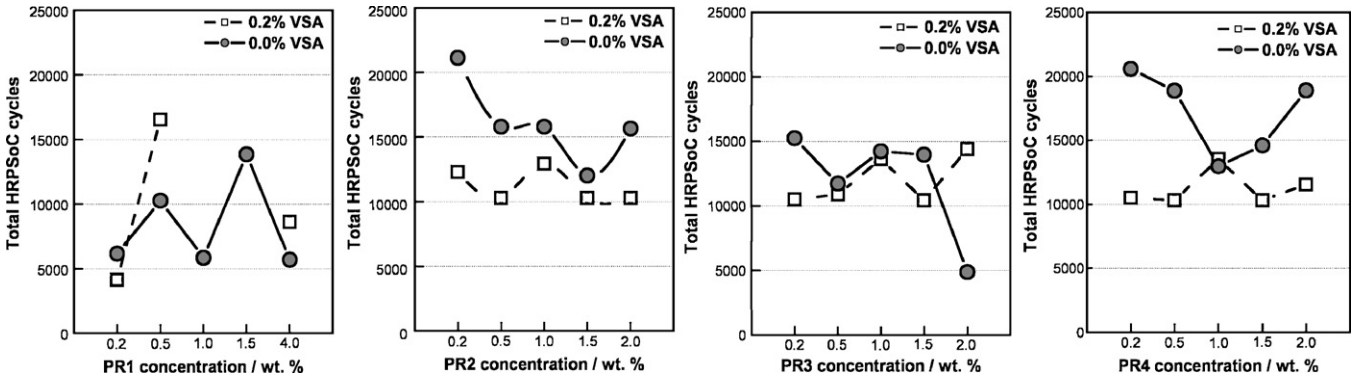

Fig. 8. Total number of completed HRPSoC cycles versus PR carbon concentration in NAM for cells with and without VS-A.

tion of 0.5% or 1.5%, whereas the PR3 additive yields cell cycle life better than 4000 cycles per cycle-set if its content in NAM is within the range from 0.2% to 1.5%.

The cells without VS-A have a different behaviour during the two cycle-sets of the HRPSoC test than their VS-containing counterparts. This difference can be clearly seen in Fig. 8 presenting the total number of completed HRPSoC cycles as a function of Printex concentration in NAM.

The cells with PR2 or PR4, at all concentration levels, complete more cycles during the two cycle-sets when no VS-A is added. In the case of PR1 and PR3 additives, however, only certain loads of these carbons yield somewhat better cell cycle life in the absence of VS-A than when VS-A is also added. Obviously, VS-A exerts an influence on the charge–discharge processes that occur within one micro-cycle of 60 s discharge and 60 s charge of the HRPSoC cycling test.

In an attempt to follow the processes that proceed during charge of cells with or without VS, the discharge was carried out for 20, 40 or 60 s, which corresponds to 1%, 2% or 3% depth of discharge (DoD), respectively. The re-charge after the above discharges was conducted with the same currents and the same durations. The obtained polarization curves are presented in Fig. 9.

The first conclusion that can be drawn from the obtained results is that the cells without VS-A undergo the same polarization during charge and discharge irrespective of the DoD. The measured polarization of the cells with VS-A is the same during all three discharges to different DoD levels, which indicates that VS-A does not affect the discharge process when conducted to 1%, 2% or 3% DoD. It has an impact on the charge process.

Thus, at 1% DoD, the negative plates undergo rapid polarization after only 15 s of charge. At 2% DoD, polarization of the negative plates starts after 30 s of the subsequent re-charge, and at 3% DoD the plates are polarized after 55 s of charge.

A similar behaviour is also observed with the cells with PR3 additive, which implies that cell polarization is a result of the effect of Vanisperse and the degree of polarization depends on

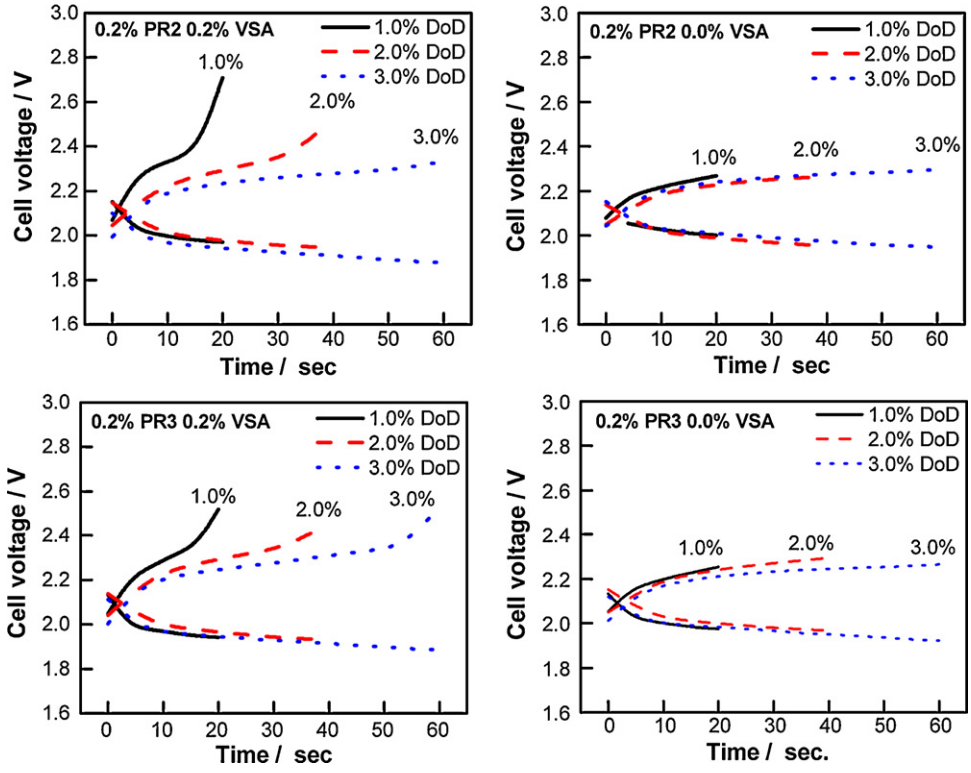

Fig. 9. Cell voltage vs. time of discharge to 1%, 2% or 3% DoD and subsequent re-charge with the same current (2*C* A) and duration for cells with PR2 or PR3, with or without VS-A, in NAM.

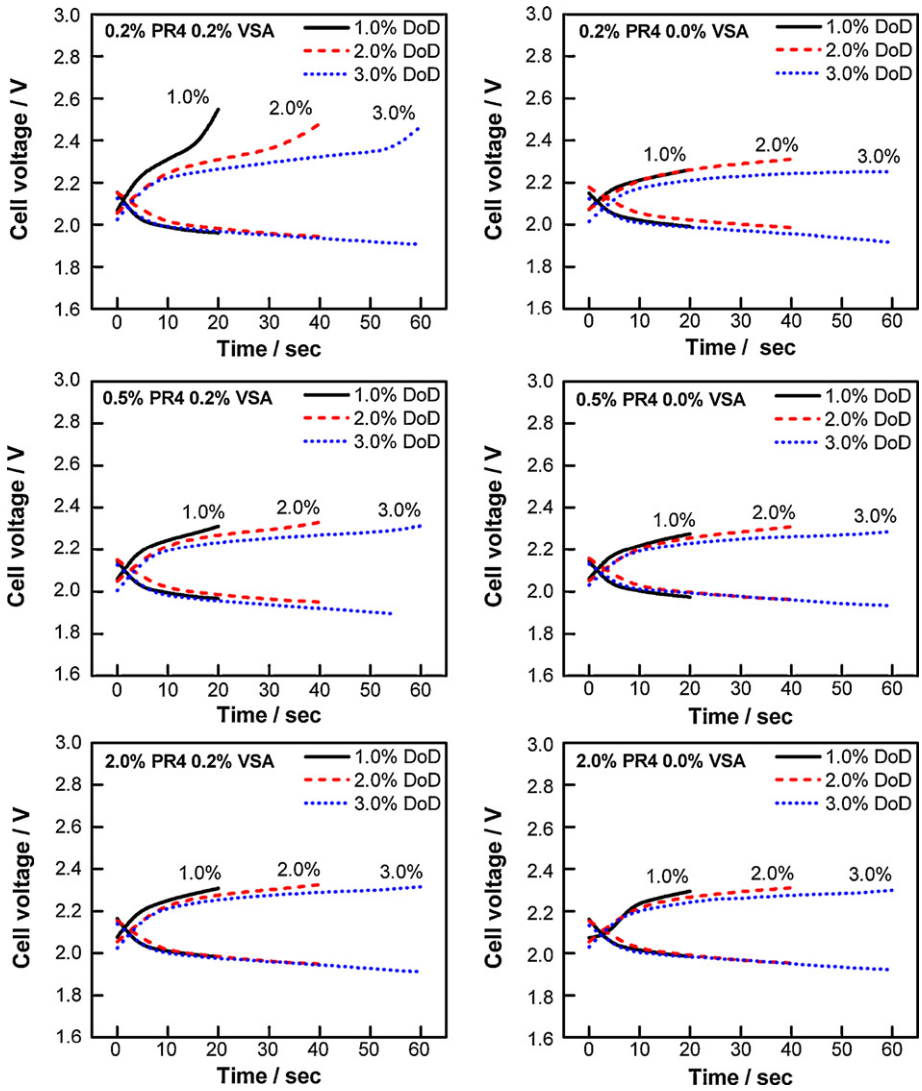

Fig. 10. Cell voltage vs. time of charge and discharge for cells with different loads of PR4 carbon in the negative plates, with or without VS-A, when discharged to 1%, 2% or 3% DoD.

the size of electrode surface area that has been cleared of the adsorbed VS layer during the discharge. The longer the discharge, the closer the charge–voltage curve to that for cells without VS-A.

The observed electrode behaviour on charge and discharge indicates that VS-A molecules are in dynamic state in NAM on cell cycling. During charge, they are adsorbed onto the lead and carbon surfaces, and then desorb leaving free (Pb + C) surfaces during discharge.

If the proposed dynamic mechanism by which VS influences the charge processes on the negative plates is true, it follows that polarization of the negative plates depends on the amount of PR additive in NAM. At constant VS content in NAM, increase of the load of PR additive will contribute to increasing the electrochemically active surface. Above certain PR concentration, VS molecules will be insufficient to cover the whole electrode surface. In this case, no electrode polarization will occur during charge because the charge reactions will continue on the VS-free Pb and C surfaces.

These processes are experimentally illustrated by the obtained polarization curves for electrodes with 0.2%, 0.5% or 2.0% PR4, presented in Fig. 10.

At 0.2% PR4 loading level, VS covers the whole electrochemically active surface of the electrode and the latter is polarized. When the electrodes contain 0.5% or 2.0% PR4, no polarization of the cells is observed, because some of the electrode surface remains free of adsorbed VS layer. The specific surface of the PR4 carbon black is 300 $m^2 g^{-1}$. This experimental finding "opens a window" for the development of a technology for effective charge with high currents by selecting an appropriate proportion between the amounts of PR and VS-A added to the negative pastes. Thus, maximum cycle life performance will be guaranteed for cells intended for HRPSoC cycling duty, but also for deep-discharge cycling modes at lower currents.

3.2. Electrochemically active carbons: AC1, AC2, AC3, and AC4

The influence of active carbon (AC) additives to the negative plates on the performance of the cells under HRPSoC cycling conditions has been extensively investigated in our laboratory during the last several years [13]. Based on the obtained results we have established that the electrochemical reaction of $PbSO_4$ reduction to Pb proceeds not only on the lead surface, but also on the surface of carbon particles. We have called these carbon forms *electrochemically active carbons* and the mechanism by which they influence the electrochemical reactions on the negative plates: *parallel mechanism of charge*. The obtained cycling test results for cells with addition of

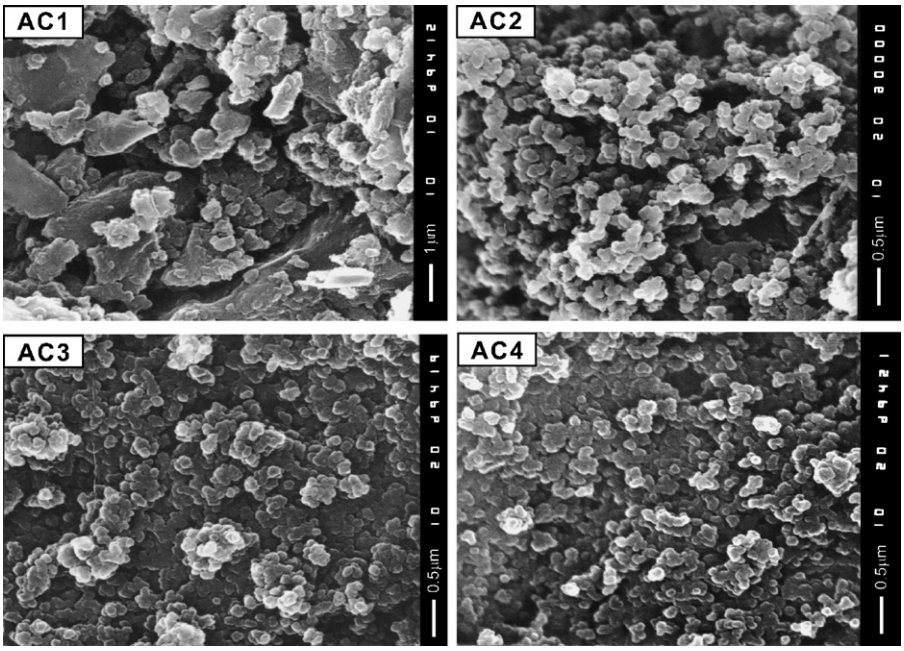

Fig. 11. SEM micrographs of the structure of active carbons AC1 to AC4.

active carbons and $BaSO_4$, with or without VS-A, will be discussed further in this paper.

3.2.1. Structure of AC particles

Fig. 11 shows SEM pictures of the structure of the four types of electrochemically active carbons labeled AC1 to AC4.

AC2, AC3 and AC4 carbons have small-sized particles. AC1 comprises mostly particles within the micro-scale region, but there are a great number of nano-sized particles, too. Table 3 presents the particle sizes of active carbons measured from the SEM images in Fig. 11. These values are several times higher than the particle size data given in the manufacturers' specifications. A more careful examination of the particles evidences that these are in fact small agglomerates of coalesced smaller particles. The connections between these smaller particles are also clearly seen in the SEM pictures. Transmission electron microscopy of the active carbons evidences analogous structure to that of the Printex particles.

SEM images of NAM with different loads of each of the four AC additives were presented in a previous paper of ours [13]. The electrical parameters of cells with AC + $BaSO_4$ + VS-A in NAM were also discussed in this publication.

3.2.2. HRPSoC cycling tests of cells with active carbon (AC1-4) and $BaSO_4$ additives to NAM, with or without VS-A

Fig. 12 presents the number of completed HRPSoC cycles, within two cycle-sets, for cells with different amounts of AC1-4 additives, with or without VS-A. The measured end-of-charge and end-of-discharge cell voltages during the first cycle-set are also given in the figure. All cells contain 0.8% $BaSO_4$ as well.

The data in the figure evidence that the cells with AC1 or AC2 without VS-A complete twice more micro-cycles within the first cycle-set than their counterparts with VS-A, the beneficial effect of these active carbon forms being more pronounced at 0.5% than at 2.0% concentration of the additive in NAM. The cells with AC3, both with and without VS-A, complete equal number of micro-cycles during the second cycle-set, at AC3 loading levels of 0.5% and 1.0%. When 0.5% AC4 is added to the negative paste, the number of completed cycles within the first cycle-set is the same for both cells with and without VS-A. However, during the second cycle-set the cell with 0.5% AC4 and VS-A completes much less micro-cycles than during the first cycle-set, whereas the cell without VS-A sustains its cycle life performance.

The graphs showing the changes in cell voltage during HRPSoC cycling evidence that it is the discharge voltage of the cells that limits the first cycle-set of the test. These results indicate that the number of completed cycles within the first cycle-set is limited by sulfation of the negative plates.

All cells under test, with and without VS-A, have a cell voltage equal to or lower than 2.4 V. On grounds of the conclusions about the effect of VS-A in cells with PR additives, it follows that addition of 0.2% VS-A is not sufficient to cover the whole surface of Pb and AC particles, and hence cannot impede the charge processes and lead to negative plate polarization. Cells with AC additives and VS-A endure far less micro-cycles than VS-free cells. This implies that VS-A impairs the reversibility of the charge–discharge processes on HRPSoC cycling, which is the reason for the smaller number of completed cycles by the cells with AC and VS-A in NAM. This effect of VS-A differs in strength depending on the type of active carbon added, being very strong in cells with AC1, AC2 or AC3, and weak in cells with AC4 additive. Probably, this difference is related to the ratio between the (Pb + C) surface area covered by adsorbed VS-A polymer molecules and the VS-free surface.

Table 3
Particle sizes of active carbons measured from the SEM images in Fig. 11.

Product	Signature	Carbon particle size range	Average carbon particle size
NORIT AZO	AC1	160–210 nm	185 nm
VULCAN XC72R	AC2	150–170 nm	160 nm
Black Pearls 2000	AC3	100–130 nm	115 nm
PRINTEX® XE2	AC4	100–130 nm	115 nm

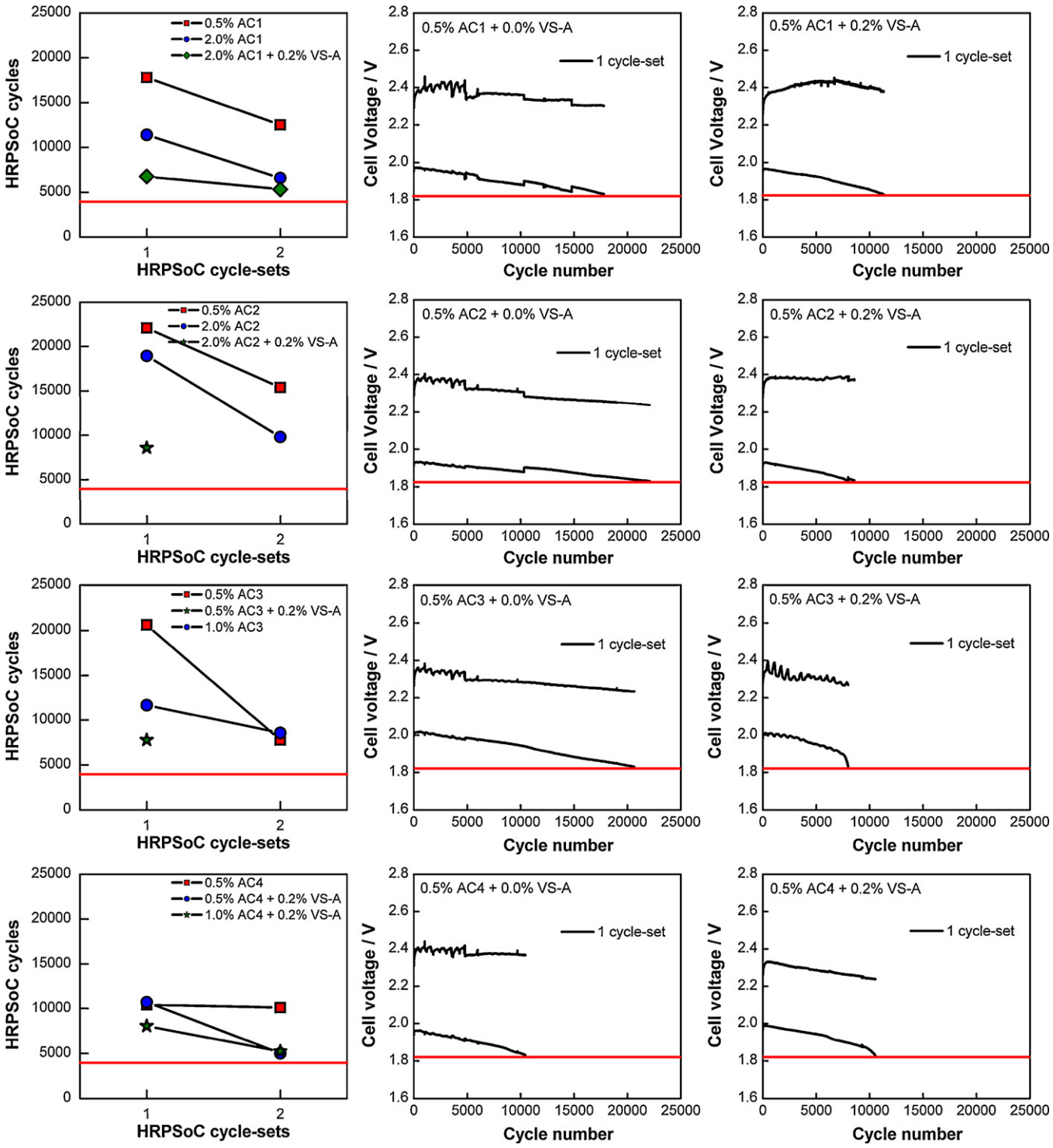

Fig. 12. Completed HRPSoC cycles, within two cycle-sets, and changes in cell voltage on cycling of cells with different amounts of AC1-4 in NAM, with or without VS-A.

Fig. 13 presents the total number of completed HRPSoC cycles by cells with two concentrations of AC3 in NAM, without VS-A, for five cycle-sets of the test. The cell capacities after each of the five cycle-sets and the measured end-of-charge and end-of-discharge voltages are also given in the figure.

While all cells reach the conditional lower cycle life limit of 4000 micro-cycles per cycle-set after five cycle-sets, the capacity of the cell with 0.2% AC3 falls below the end-of-life criterion of 70% of the rated value already after three cycle-sets, and that of the cell with 1.0% AC3 after four cycle-sets. These results suggest that it is not quite appropriate to apply the same end-of-life criterion to all types of lead-acid batteries.

Fig. 14 summarizes the experimental data about the effect of the three types of expander components on cell cycle life performance, presented in terms of total number of completed micro-cycles during the HRPSoC cycling test.

The best cycle life performance is registered for the cells with a combination of AC and $BaSO_4$ in NAM, the maximum number of completed cycles depending mostly on the type and content of AC added, but the amount of $BaSO_4$ being of importance, too.

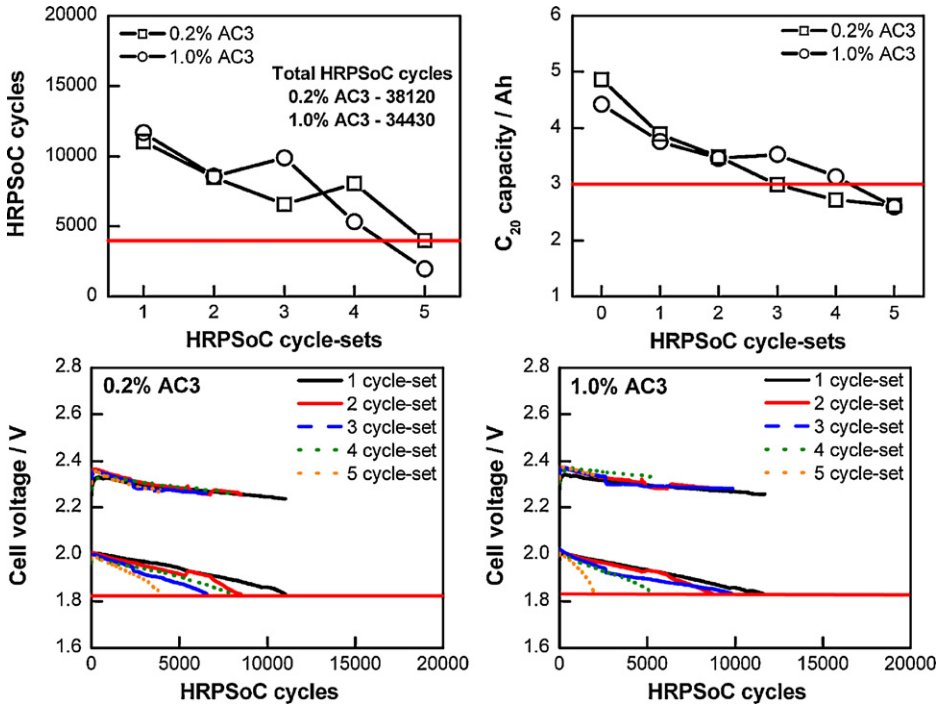

Fig. 13. Total number of completed HRPSoC cycles, end-of-charge and end-of-discharge cell voltages and C_{20} capacity of cells with 0.2% or 1.0% AC3 in NAM for five cycle-sets of the HRPSoC test.

The cells with AC alone (e.g. AC3) have shorter cycle life, which comes to indicate that $BaSO_4$ exerts its own specific effect on the HRPSoC behaviour of the cells by improving the reversibility of the charge–discharge processes. VS-A, on the other hand, has the opposite effect, i.e. it shortens the cycle life of the cells in the HRPSoC duty.

3.2.3. *Influence of AC on the capacitive and Faraday current components on voltammetric scanning of model electrodes*

Fig. 15 presents the recorded volt–ampere curves for carbon, Pb and (Pb + carbon) model electrodes obtained by linear sweep voltammetry measurements between −0.5 and −1.3 V at a scan rate of 20 mV s^{-1}.

It is evident from the figure that all current–voltage electrode characteristics depend on the type of carbon additive used. The charge–discharge curves recorded on carbon electrodes are similar to those of a double layer capacitor. The AC1 carbon electrode has the lowest capacity on discharge and charge of the electric double layer, whereas the AC3 carbon electrode exhibits the highest capacity.

The increased slope of the cathodic volt–ampere curve for the AC2 and AC3 electrodes at potentials more negative than −1.1 V is probably related to reduction of hydrogen ions and incorporation of the obtained hydrogen atoms into the carbon structure without formation of hydrogen bubbles (a new phase). During the subsequent anodic polarization run, the hydrogen atoms are reduced first, which causes the pronounced hysteresis in the volt–ampere curve.

The voltammograms for the Pb electrode reflect the processes of anodic oxidation of Pb, formation of passive $PbSO_4$ layer and subsequent reduction of the $PbSO_4$ phase. This electrode behaviour corresponds to the classical electrochemical reactions of lead oxidation and reduction of $PbSO_4$ in H_2SO_4 solution.

A comparison of the obtained current–voltage curves for carbon and Pb electrodes shows that the double layer charge–discharge processes are of the order of 10 times faster than the processes involved in the electrochemical Pb reactions. Moreover, the quantity of electricity of the double layer capacitor is higher than that of the Faradaic reactions of lead oxidation and $PbSO_4$ reduction. This

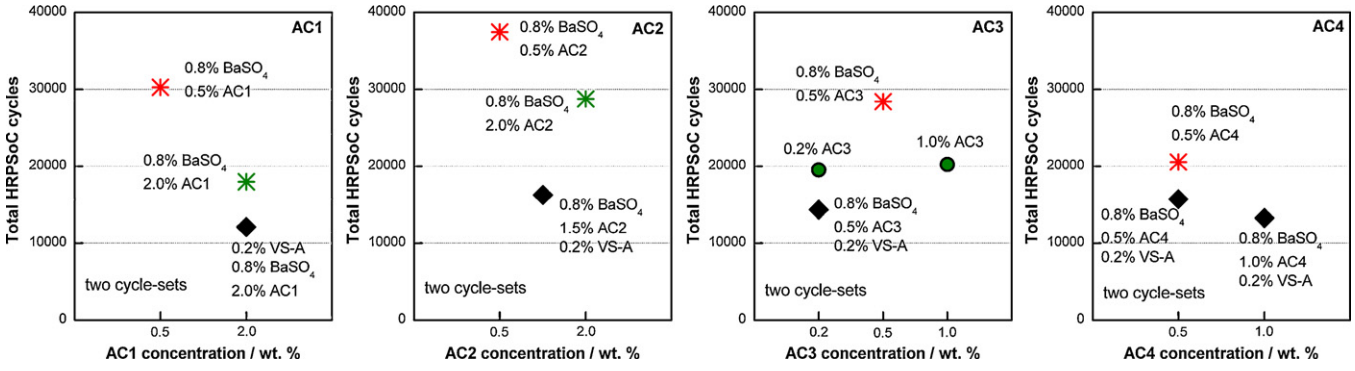

Fig. 14. Summary of the effects of the three expander components on the total number of completed HRPSoC cycles for cells with active carbons AC1-4 in NAM.

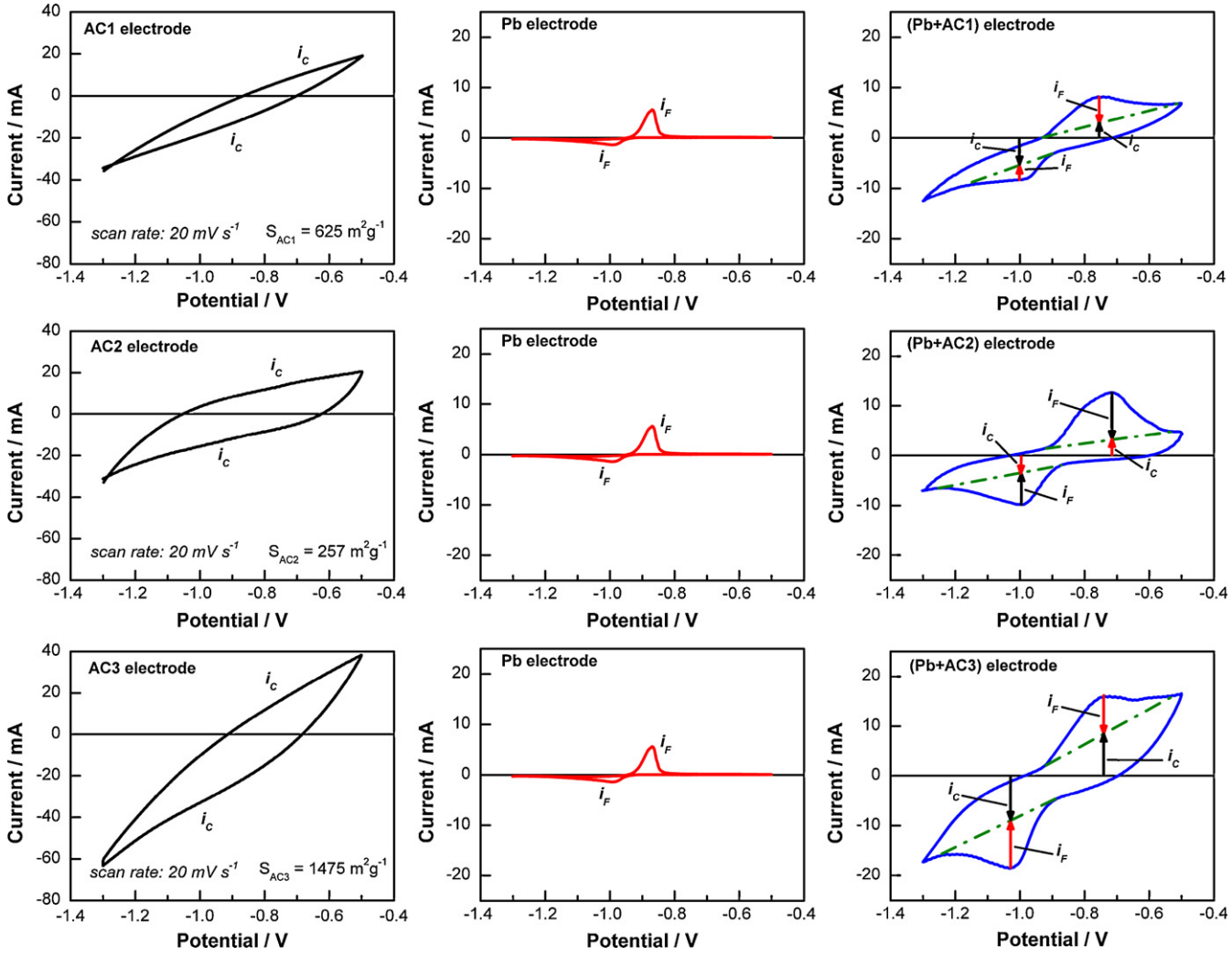

Fig. 15. Volt–ampere curves for carbon, Pb and (Pb + carbon) model electrodes obtained by cyclic voltammetry measurements between −0.5 and −1.3 V at a scan rate of 20 mV s^{-1}. 5th voltammetric cycle.

finding is logical as the surface area of the active carbons is much larger than that of the lead particles.

Fig. 15 evidences that the voltammograms for the (Pb + carbon) electrodes are similar in profile to those for the pure Pb electrode, reflecting the Faradaic reactions, but they feature higher and broader anodic and cathodic current peaks.

The volt–ampere curves for the (Pb + carbon) electrodes are a combination of the voltammograms for the carbon and Pb electrodes. The dashed lines in Fig. 15 represent the volt–ampere curves for the capacitive part of the (Pb + AC) electrodes. These are similar to the volt–ampere curves recorded on the carbon electrodes and reflect only the capacitive current component. These capacitive currents are lower in value than the currents of the carbon electrodes, because of the smaller amount of carbon contained in the (Pb + C) electrodes than in the pure carbon electrodes. Both the capacitive and Faradaic current components are marked in the curves for the (Pb + C) electrodes. A comparison between the currents flowing through the Pb and (Pb + C) electrodes shows that the cathodic current at the maximum of the Faradaic reduction of $PbSO_4$ to Pb is much higher on the (Pb + C) electrode than on the Pb electrode. This suggests that the reaction of $PbSO_4$ reduction proceeds on the carbon surface of the (Pb + C) electrode as well. Hence, the Faradaic reaction of Pb^{2+} ion reduction to Pb proceeds on the carbon surface, too, which improves the efficiency of charge of the negate plates.

An analogous interpretation of the anodic current components, reflecting the processes of Pb oxidation to $PbSO_4$, indicates that the anodic current at the current maximum is close in value or lower than the Faradaic current component, i_F, on the (Pb + C) electrode. It seems that some Pb is deposited on the carbon surface during cycling and this Pb, too, is involved in the processes that take place within the individual micro-cycles.

The volt–ampere curves recorded on the three types of (Pb + C) model electrodes differ in profile, which indicates that the three active carbon additives have different electrochemical properties. When selecting the most appropriate carbon additives for the negative plates of batteries intended for use in hybrid electric vehicles it is essential to evaluate the degree of involvement of the particular carbon material in the Faradaic reactions on HRPSoC cycling.

These experimental findings are in support of the hypothesis that reduction of $PbSO_4$ to Pb and subsequent oxidation of Pb proceed on the AC surface parallel to the processes on the Pb surface, i.e. the parallel mechanism of charge is active.

3.2.4. Influence of carbon particle size on HRPSoC cycling performance of cells with Printex or electrochemically active carbons in NAM

The above test results indicate that each type of carbon additive to the negative plates exerts its own specific influence on the performance of lead-acid cells on HRPSoC cycling. In order to make

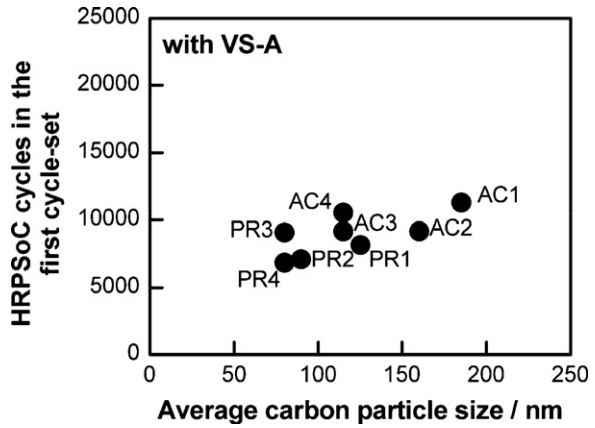

Fig. 16. Completed HRPSoC cycles within the first cycle-set vs. carbon particle size for cells with PR or AC carbons and VS-A in the negative plates.

a more clear distinction between the different carbon additives and their specific impact on cycle life performance, we will try to summarize the test results in the following way.

For each type of carbon additive we select the cell with the concentration that yields the best cycle life performance. It is interesting to see how do the sizes of the carbon particles affect the cycle life performance of the cells. We compared the maximum completed number of cycles within the first cycle-set for cells with Vanisperse against the size of the Printex and active carbon particles as summarized in Tables 2 and 3. Fig. 16 presents the obtained dependences.

When the cells contain both VS-A and carbon additives, the number of completed cycles within the first cycle-set is within the range from 7000 to 11,000 cycles. Probably, VS-A molecules incorporated in the interface structure suppress the specific effect of carbon particle size on cell cycle life and thus the influence of VS-A becomes dominating.

Fig. 17 presents the completed HRPSoC cycles within the first cycle-set as a function of carbon particle size for cells with PR or AC and $BaSO_4$, but without VS-A, in the negative plates.

It can be seen from the data in the figure that cells with PR1-4 or AC4 additives, with particle sizes ranging from 85 to 125 nm, have a cycle life of between 6500 and 12,800 cycles. The cells with AC1, AC2 or AC3 active carbons (with mean particles sizes between 115 and 185 nm) endure from 13,800 to 22,300 cycles. These results indicate that when the lead and carbon surfaces are clear of adsorbed organic surface active substance (VS-A), the specific effect of the respective carbon additive exhibits fully. The

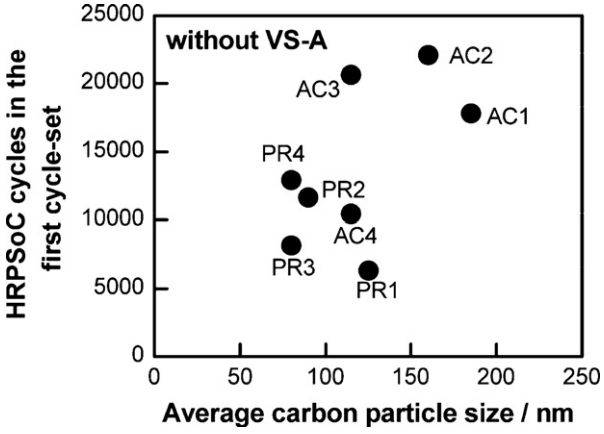

Fig. 17. Completed HRPSoC cycles within the first cycle-set vs. carbon particle size for cells with PR or AC carbons but without VS-A in the negative plates.

second parameter that affects the reversibility of the processes during charge and discharge is the type of the carbon additive. Active carbons have a stronger effect on cell cycle life than Printex carbon blacks.

4. General conclusions

4.1. Summary of the specific effects of expander components on the charge processes at the negative plates of VRLA cells on HRPSoC cycling

The overall charge process of the negative plates of a lead-acid cell involves the following elementary processes:

(a) dissolution of $PbSO_4$ crystals and formation of Pb^{2+} ions;
(b) diffusion of the Pb^{2+} ions through the solution to the lead electrode and adsorption of these Pb^{2+} ions onto the electrode surface;
(c) electron transfer through the phase interface electrode/solution and proceeding of the electrochemical reaction $Pb^{2+} + 2e^- \rightarrow Pb$;
(d) surface diffusion of Pb atoms to the growth cites of Pb crystals and incorporation of Pb atoms into the lead crystal structure.

Which elementary processes are affected by each of the three expander components, especially by the carbon additives?

- It has been established that carbon additives reduce the mean pore radius of NAM (Fig. 14 in Ref. [13]). Thus, smaller $PbSO_4$ crystals are formed, which have higher solubility and sustain higher Pb^{2+} ion concentration in the solution, thus supplying sufficient amount of Pb^{2+} ions for the charge process. The second expander component, $BaSO_4$, has a similar effect. Its particles are very small in size and provide a great number of nuclei onto which $PbSO_4$ precipitates, facilitating formation of numerous small-sized $PbSO_4$ crystals. Cycling test results have proved that $BaSO_4$ loading level of 1% ensures the best cycle life performance of lead-acid cells on HRPSoC cycling [14].
- Diffusion of Pb^{2+} ions and their adsorption on the electrode surface are relatively fast processes, because of the high acid concentration gradient created at the electrode surface as a result of the electrochemical reaction.
- Carbon particles adsorb onto the lead surface, mostly to the edges and apexes of the lead crystals, and at higher carbon concentrations, onto the crystal surface as well (Fig. 5). Depending on the structure and properties of the carbon additive used, the contact carbon/lead may vary in stability. Some of the carbon types have a stable and low-ohmic contact with the lead surface. These carbon additives will guarantee good electrochemical behaviour of the (Pb + C) electrode.
- The carbon phase may have different electric conductivity. Highly conductive carbon additives yield an electric double layer at the interface carbon/solution (Fig. 15, carbon electrode). Thus, the carbon surface contributes to increasing the electrochemically active surface on which the charge processes proceed (the specific surface of lead is about 0.5 $m^2\ g^{-1}$ and that of carbon is tens or hundreds times higher).
- The electrochemical reaction $Pb^{2+} + 2e^- \rightarrow Pb$ proceeds at the (Pb + C) surface (Fig. 15, (Pb + C) electrode). The increased electrode surface sustains low electrode polarization and thus prevents the hydrogen evolution reaction to proceed, thus improving the charge efficiency of the negative electrode (Figs. 12 and 13). The reversibility of the charge–discharge processes increases and so does the cycle life of the cells (batteries) in the HRPSoC duty.

- The surface active component of the expander (lignosulfonate) is adsorbed on the (Pb + C) surface, which creates a high potential barrier for the electron transfer through the phase interface and hence retards the electrochemical reaction of Pb^{2+} ion reduction. For this reaction to proceed, the cathodic electrode potential should increase on charge (Fig. 9). This triggers the hydrogen evolution reaction, which impedes strongly the charge efficiency. The reversibility of the processes during charge and discharge is reduced leading to progressive sulfation of the negative plates. Therefore, addition of surface active substances should be avoided, if possible, or they should be introduced but in minimum amounts (Fig. 11).

These are in brief the specific effects of the individual expander components, and especially of carbons, on the mechanism of the charge processes in a lead-acid cell on HRPSoC cycling.

Acknowledgements

The authors acknowledge with gratitude the financial support provided by the Advanced Lead-Acid Battery Consortium (ALABC Project No. C2.3). We want to express our special thanks to Dr. Patrick Moseley and Dr. David Prengaman for encouraging the present investigation. This paper was reported at the ALABC Member's and Contractor's Conference 2009.

References

[1] D. Pavlov, J. Electrochem. Soc. 139 (1992) 3075.
[2] K. Nakamura, M. Shiomi, K. Takahashi, M. Tsubota, J. Power Sources 59 (1996) 153.
[3] M. Shiomi, T. Funato, K. Nakamura, K. Takahashi, M. Tsubota, J. Power Sources 64 (1997) 147.
[4] A.F. Hollenkamp, W.G.A. Baldsing, S. Lau, O.V. Lim, R.H. Newnham, D.A.J. Rand, J.M. Rosalie, D.G. Vella, L.H. Vu, ALABC Project N1.2, Annual Report, July 2000–June 2001.
[5] M. Calabek, K. Micka, P. Krivak, P. Baca, J. Power Sources 158 (2006) 864.
[6] L.T. Lam, C.G. Phyland, D.A.J. Rand, D.G. Vella, L.H. Vu, ALABC Project N3.1, Final Report, 2002, June.
[7] R.H. Newnham, W.G.A. Baldsing, A.F. Hollenkamp, O.V. Lim, C.G. Phyland, D.A.J. Rand, J.M. Rosalie, D.G. Vella, ALABC Project C/N 1.1, Final Report, July 2000–June 2002.
[8] S.V. Baker, P.T. Moseley, A.D. Turner, J. Power Sources 27 (1989) 127.
[9] L.T. Lam, R. Louey, J. Power Sources 158 (2006) 1140.
[10] L.T. Lam, R. Louey, N.P. Haigh, O.V. Lim, D.G. Vella, C.G. Phyland, L.H. Vu, J. Furukawa, T. Takada, D. Monma, T. Kano, J. Power Sources 174 (2007) 16.
[11] L.T. Lam, N.P. Haigh, C.G. Phyland, D.A.J. Rand, International Patent Number WO 2005/027255 AL.
[12] P.T. Moseley, J. Power Sources 191 (2009) 134.
[13] D. Pavlov, T. Rogachev, P. Nikolov, G. Petkova, J. Power Sources 191 (2009) 58.
[14] D. Pavlov, P. Nikolov, T. Rogachev, J. Power Sources (2009), doi:10.1016/j.j.powsour.2009.11.060, this issue.
[15] G. Petkova, D. Pavlov, J. Power Sources 113 (2003) 355.
[16] V. Iliev, D. Pavlov, J. Appl. Electrochem. 15 (1985) 39.